ACS Catalysis

Research Article

pubs.acs.org/acscatalysis

Radical Mechanism of Isocyanide-Alkyne Cycloaddition by Multicatalysis of Ag_2CO_3, Solvent, and Substrate

Pin Xiao, Haiyan Yuan, Jianquan Liu, Yiying Zheng, Xihe Bi,* and Jingping Zhang*

Faculty of Chemistry, Northeast Normal University, Changchun 130024, China

Supporting Information

ABSTRACT: A combined DFT and experimental study was performed to reveal the mechanism of isocyanide-alkyne cycloaddition. Our results indicate that the mechanism of this valuable reaction is an unexpected multicatalyzed radical process. Ag_2CO_3 is the pivotal catalyst, serving as base for the deprotonation of isocyanide and oxidant to initiate the initial isocyanide radical formation. After the cycloaddition between isocyanide radical and silver-acetylide, substrate (isocyanide) and solvent (dioxane) replace the role of Ag_2CO_3. They act as a radical shuttle to regenerate isocyanide radical for the next catalytic cycle, simultaneously completing the protonation. Furthermore, the bulk solvent effect significantly increases the reactivity by decreasing the activation barriers through the whole reaction, serving as solvent as well as catalyst.

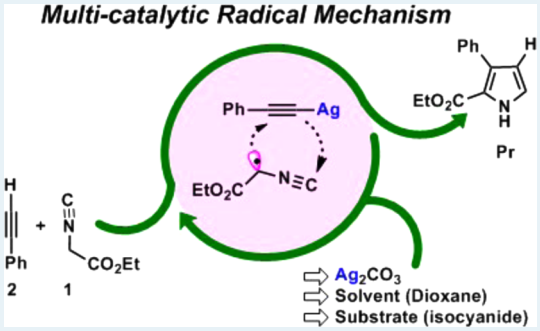

KEYWORDS: *Ag_2CO_3, DFT, multicatalysis, pyrrole, radical mechanism*

INTRODUCTION

Pyrrole and their derivatives have wide applications in the fields of material sciences,[1] agrochemicals,[2] natural products,[3] and pharmaceuticals.[4] Consequently, methods to synthesize heterocycles, such as pyrroles, have attracted increasing interest in organic chemistry.[5] The application of transition-metal-catalyzed C−H bond activation has revolutionized this field.[6] However, synthetic methods reported so far largely depend on elaborately designed substrates that are not readily available. Recently, silver-catalyzed synthetic methods of electron-withdrawing compounds and nonactivated terminal alkynes to access pyrroles have evolved as an effective strategy.[7−9] In particular, the Lei group[7] and the Bi group,[8] our co-workers, have separately discovered the unique catalytic activity of Ag_2CO_3 capable of efficiently catalyzing the isocyanide[10,11]-alkyne cycloaddition to pyrroles (Scheme 1). This discovery has addressed a long-term challenging issue that nonactivated terminal alkynes cannot take part in this [3 + 2] cycloaddition, thus establishing a fundamental reaction. However, the exact reaction mechanism remains unclear. Furthermore, the computational investigations on the silver-catalyzed reactions are still rather scarce hitherto. Therefore, we herein devote our efforts to uncover the reaction mechanism by combined DFT and experimental studies.

Scheme 1. Mechanistic Proposals for Ag_2CO_3-Catalyzed Isocyanide-Alkyne Cycloaddition

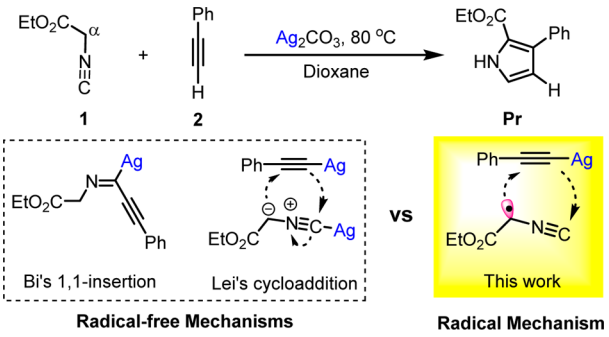

Two possible radical-free mechanisms including the 1,1-insertion of isocyanide to C−Ag bond and the cycloaddition of silver-acetylide with silver-isocyanide, were proposed by the Bi[8] and Lei groups,[7] respectively (Scheme 1). Neverthless, a careful inspection of the structure for substrate ethyl isocyanoacetate (**1**) suggests that the C^{α} is connected by two electron-withdrawing −NC and carbonyl groups, thereby the C^{α} is highly activated.[10] Hence, the C^{α} easily becomes a radical, and this [3 + 2] cyclization reaction may proceed through a radical mechanism wherein substrate **1** is a potential radical source. To certify this speculation, we conducted experiments with radical scavengers such as BHT (3,5-di*tert*-butyl-4-hydroxytoluene) and TEMPO ((2,2,6,6-tetramethyl-piperidin-1-yl)oxyl) under standard conditions (Table S1). No reaction occurred, and only **2** and solvent were detected by TLC, indicating that **1** completely disappeared. To exclude the possibility of scavenger reacting with Ag(I) salt, we conducted ^{1}H NMR spectroscopy analyses for pure BHT before or after adding Ag_2CO_3. No obvious shift was observed for the characteristic peaks of BHT after adding Ag_2CO_3, suggesting that BHT has no effect on the

Received: June 15, 2015
Revised: August 28, 2015
Published: September 10, 2015

DOI: 10.1021/acscatal.5b01703
ACS Catal. 2015, 5, 6177−6184

catalytic activity of Ag_2CO_3 in the current reaction. Furthermore, a thin silver mirror on the wall of the reaction vessel was observed under the standard reaction conditions (see SI-i). Thus, these results confirmed that the reaction proceeded through a radical process in which **1** is the potential radical source. As expected, the radical mechanism was subsequently further confirmed by our computational calculations, which is more favorable than the radical-free ones previously proposed by Lei[7] and Bi groups.[8] Previously, a similar radical mechanism for the formation of furans was reported by Stirling et al.,[12] wherein Ag_2CO_3 is stoichiometric, and the formation of radical is a silver-consumed process. However, Ag_2CO_3 is in a catalytic amount in the current reaction, thus implying other species may act as radical shuttle following the initial radical formation by Ag_2CO_3. Consequently, several key questions were proposed as follows: (a) is it possible for substrate or solvent 1,4-dioxane[13] (**S**) to initiate radical formation? (b) what is the effective catalyst in the catalytic cycle, single or multiple? and (c) which specie provides the proton for protonation and/or H-shift: $AgHCO_3$ or extra assistant,[14] such as substrate,[15] solvent,[16] or trace water?[17] Timely mechanistic rationalization would help exploit the potential of such silver-catalyzed multicomponent synthetic methodologies. Therefore, we performed a DFT study to investigate the detailed reaction mechanism, considering the aforementioned questions.

COMPUTATIONAL DETAILS

All calculations were performed using Gaussian 09 package.[18] Geometries were optimized using B3LYP[19] density functional with a basis set of LANL2DZ + f (1.611)[20] for Ag and 6-31G (d, p) basis set for other atoms in gas phase considering calculation cost and practical possibility for the size of investigated system. Single-point energies were calculated with M06[21]/SDD-6-311++G (d, p),[22] which was generally considered to be more accurate for Ag-containing reaction and could give reasonable agreement with higher-level calculations.[23] Calculations for radical species employed the unrestricted open-shell computational method, and the resultant relative errors of spin contamination were less than 3.2% in the current study. Frequency calculations at the same level were performed to verify the stationary points to be real minima or saddle points and to obtain thermal energy corrections at 353.15 K. Intrinsic reaction coordinates (IRC)[24] were carried out to verify whether the optimized transition state (**TS**) structures connected the correct reactant and product or not on the potential energy surface. Solvent (1,4-dioxane) effects were calculated by using the new SMD solvation model.[25] All charge distributions were calculated by Natural Bond Orbital (NBO) analysis.[26] The strength of intermolecular interactions was evaluated using the topology analysis techniques by Multiwfn[27] software. Computed structures are illustrated using CYLView[28] and nonessential hydrogen atoms are omitted for clarity. All energies reported here are in kcal/mol, and bond lengths are in angstroms (Å).

RESULTS AND DISCUSSION

As displayed in Scheme 2, the calculated results indicate that the cycloaddition of **1** and phenylacetylene (**2**) is a stepwise process involving (I) the deprotonation followed by oxidation of isocyanide by Ag_2CO_3 to form isocyanide radical **4** (in yellow), (II) the intermolecular cycloaddition between **4** and silver-acetylide (in pink), (III) the concerted protonation and

Scheme 2. Catalytic Cycle of the Favorable Radical Mechanism for the Title Reaction

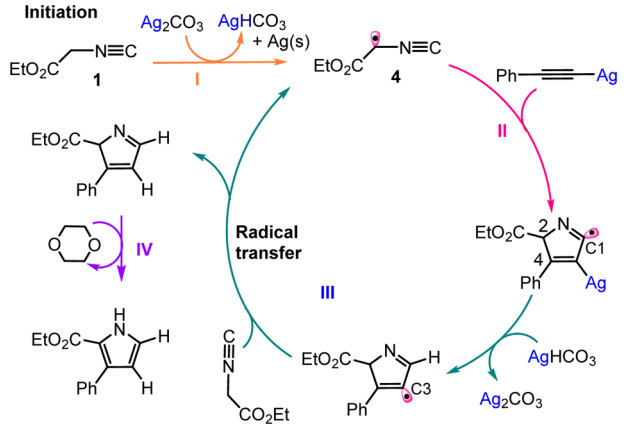

regeneration of isocyanide radical (in olive), and finally (IV) the H-shift leading to an aromatic pyrrole as product (in violet). The rate-determining step (**RDS**) is the first C2−C4 bond formation with a free-energy barrier ($\Delta\Delta G^{\ddagger}$) of 10.2 kcal/mol in process II.

For process I, two types of mechanisms were investigated for the formation of **4** initiated by **1** and **S** with Ag_2CO_3, considering unassisted (path I-1/2) and various numbers of solvent-assisted (denoted as n**S**-assisted, n = 1−3, path I-1/2-n**S**) processes, respectively (Figures 1 and 2). For the initiation by **1** case, computed results indicate that **nS**-assisted pathways (path I-1-n**S**) are more favorable than the unassisted one (path I-1), and the 3**S**-assisted (path I-1-3**S**) is the most favorable process. In this process, two **S** molecules coordinate to Ag1 and another one to Ag2 (Figure 1, in black), meeting the four-coordinated Ag ions.[29] The reaction starts from the deprotonation of substrate **1** by Ag_2CO_3 acting as base with 3**S** assistant. H1 of **1** transfers from C^{α} to O1 of Ag_2CO_3 with a $\Delta\Delta G^{\ddagger}$ value of 7.7 kcal/mol via a six-membered transition state **TS(1−3)-3S** to form zwitterionic intermediate **3−2S** and $AgHCO_3$-**S**. The further oxidation of isocyanide anion of **3−2S** by Ag^+ ion yields isocyanide radical **4** and Ag-2**S** exothermically. This is in good accordance with the experimental observation of silver mirror phenomenon (SI-i). As shown in Figure 1, the formation of **4** is kinetically and thermodynamically favorable. The relative free energy (ΔG) of **TS(1−3)-3S** is −9.7 kcal/mol lower than those of **TS(1−3)** and other **TS(1−3)-nSs** by 22.7 and 1.9−8.5 kcal/mol, respectively. The coordination of **S** significantly stabilizes the structure of **TS(1−3)-3S** via Ag···O coordinations and C−H···O intermolecular hydrogen bonds, thus dramatically improves reaction activity.

For solvent **S** as the radical initiator to generate **4** case, the ΔG value of starting material (**S** + Ag_2CO_3) is set as the reference zero of the energy herein. The location of transition states for the deprotonation of **S** shows similar observation as initiated by **1** case that Ag prefers to be four coordinated and **TS(S−S$^{\bullet}$)-3S** is the most favorable one by 19 and 4.1−5.9 kcal/mol compared with **TS(S−S$^{\bullet}$)** and other **TS(S−S$^{\bullet}$)-nSs**. Along with the release of $AgHCO_3$, assistant **S**, and silver atom by self-redox, **S**$^{\bullet}$[30] is located on 3.2 kcal/mol of relative free energy. In the next step, **S**$^{\bullet}$ forms a complex with substrate **1** (**S**$^{\bullet}$ + **1**) that proceeds through a transition state **TS(S$^{\bullet}$−S)** with a $\Delta\Delta G^{\ddagger}$ value of 6.0 kcal/mol to yield radical **4** and **S** exothermally. Considering the reaction temperature (353.15 K), the value for the deprotonation of **S** lies in the acceptable

DOI: 10.1021/acscatal.5b01703
ACS Catal. 2015, 5, 6177−6184

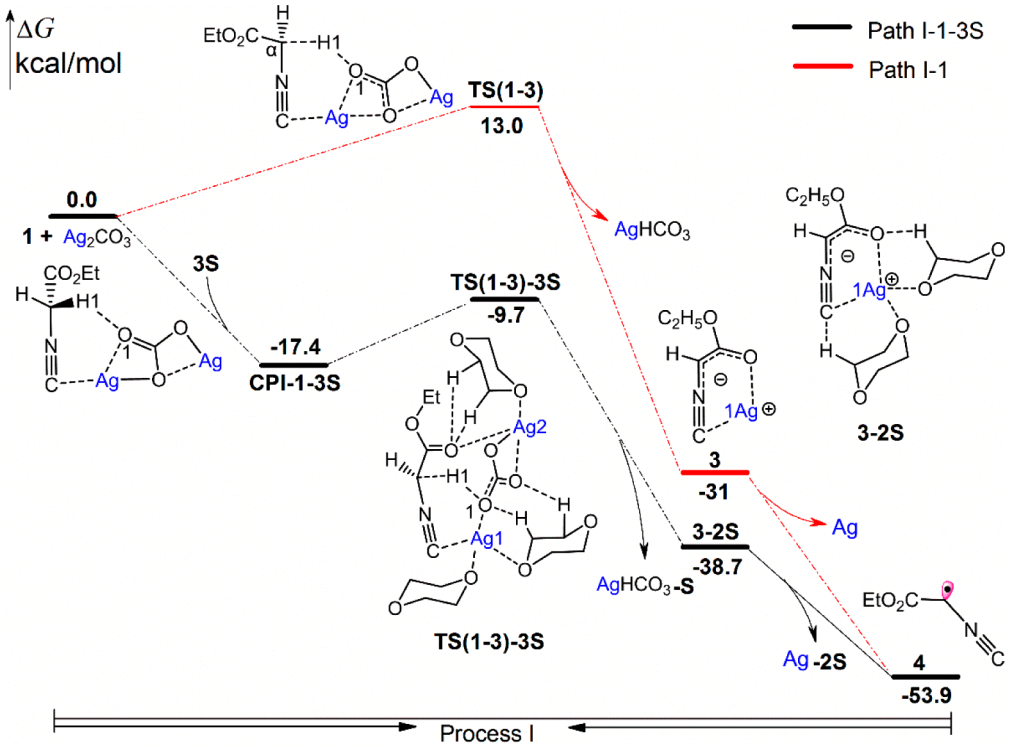

Figure 1. DFT-computed free-energy (ΔG_{sol}, in kcal/mol) profile for the formation of **4** initiated by **1** with Ag_2CO_3 in unassisted (path I-1) and 3**S**-assisted (path I-1-3S) pathways.

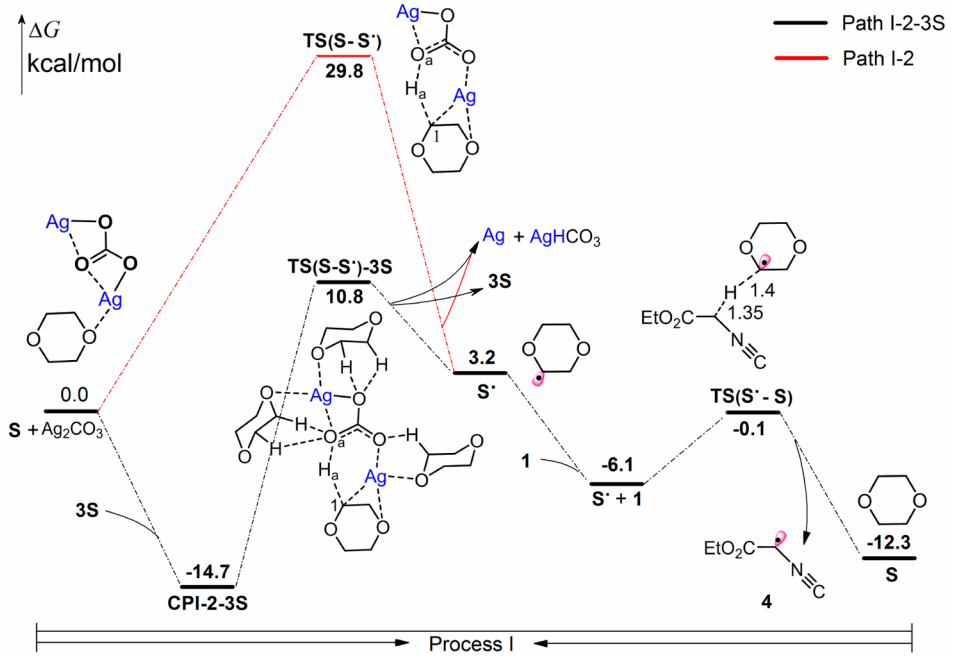

Figure 2. DFT-computed free-energy (ΔG_{sol}, in kcal/mol) profile for the formation of **4** initiated by **S** with Ag_2CO_3 in unassisted (path I-2) and 3**S**-assisted (path I-2-3S) pathways.

range ($\Delta\Delta G^{\ddagger}$ = 25.5 kcal/mol). Notably, **S**$^{\bullet}$ can easily initiate **1** to form **4** via **TS(S**$^{\bullet}$**−S)** with a low $\Delta\Delta G^{\ddagger}$ value of 6.0 kcal/mol. Thereby, process I can be promoted dramatically by bulk solvent, in which **S** plays as not only solvent but also catalyst. The comparison of the free energies shown in Figures 1 and 2 suggests that the generation of radical **4** initiated by **1** with Ag_2CO_3 is predominant. It is attributed to the fact that C^{α} atom of **1** is connected by two strong electron-withdrawing groups—NC and carbonyl—those strengthen the acidity/dissociation of C^{α}−H.

In the following intermolecular cyclization process II, three possible pathways are examined: radical **4** reacts with silver-acetylide **5** in **S**-assisted (path II-1)/unassisted (path II-2) pathways or phenylacetylene **2** (path II-3) to provide the five-membered cyclic intermediate **10** or **11**. The DFT-computed Gibbs free-energy profile of the most favorable path II-1 is

DOI: 10.1021/acscatal.5b01703
ACS Catal. 2015, 5, 6177−6184

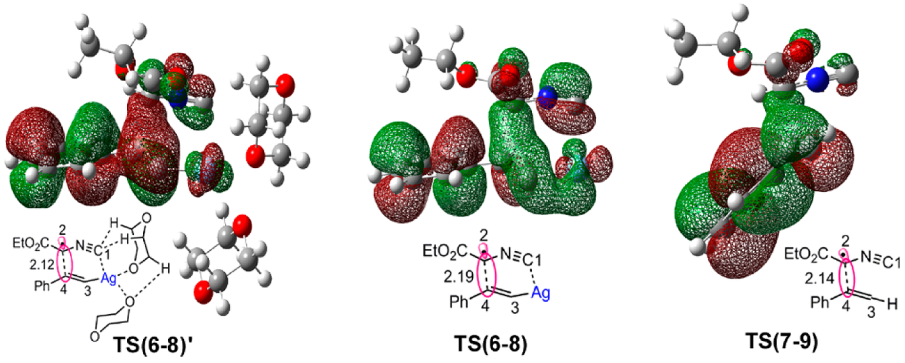

Figure 3. HOMO−1s of **TS(6−8)′**, **TS(6−8)**, and **TS(7−9)** for C−C bonds formation (pink ellipse).

Scheme 3. Key Intermediates and Transition States along with Relative Free Energies (ΔG_{sol}, in kcal/mol) of Path III-1/III-2 in Process III (Distances Are in Å)

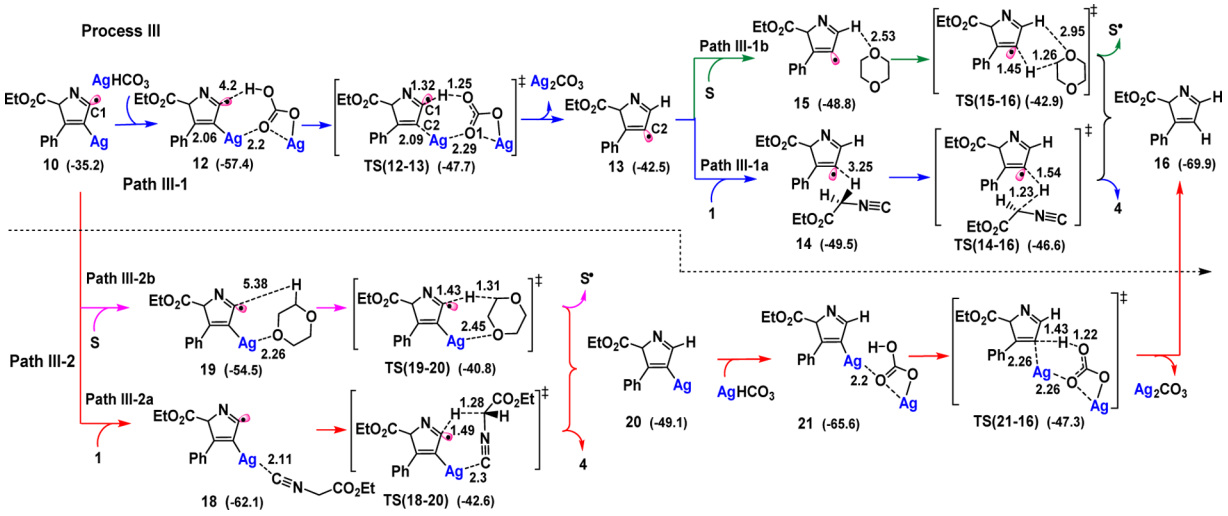

shown in Figure 3, with two molecules of **S** coordinating with Ag, and those of paths II-2/-3 are presented in Figure S4. These three pathways are a stepwise C−C bond formation process and C2−C4 bond forms preferentially than C1−C3 bond, via transition states **TS(6−8)′**/**TS(6−8)**/**TS(7−9)** and **TS(8−10)′**/**TS(8−10)**/**TS(9−11)** with the ΔG values of −20/−7.8/5.9 and −25.3/−9.5/−4.9 kcal/mol. The computed results indicate that the reaction of **4** with **5** is more preferred than that with **2** by 25.9 and 13.7 kcal/mol respectively, which agrees well with the experimental observation of substantial **5**. Obviously, path II-1 is the most kinetically and thermodynamically favorable, delivering Ag-containing intermediate **10** coordinated with two **S** molecules. This can be attributed to the following reasons: (1) the complex **6′** is more stable than **6** and **7** by 9.8 and 25.3 kcal/mol respectively, (2) the effective secondary orbital interaction of the reaction site (C2−C4) and the electronic delocalization in HOMO−1 of **TS(7−9)** are weaker than those in **TS(6−8)′** and **TS(6−8)** (Figure 3), (3) the negative charge on C4 (−0.192*e*/−0.208*e*/−0.067*e*) in **TS(6−8)′**/**TS(6−8)**/**TS(7−9)** indicates the strong nucleophilic ability of C4 in Ag-containing pathway, (4) the bond length of C2−C4 in **TS(6−8)′** is shorter than those in **TS(6−8)** and **TS(7−9)** (Figure 3). Hereby, we only discuss the Ag-containing pathway in the following processes III and IV.

For process III, the reaction follows two alternative pathways paths III-1 and III-2 from intermediate **10**. As depicted in Scheme 3, path III-1 undergoes protonations of C1 and C3 radicals by $AgHCO_3$ (**10** → **13**) and **1**/**S** (**13** → **16**), respectively. Intermediate **10** combines with $AgHCO_3$ to form adduct **12**. The conversion of **12** to **13** is a concerted process via a seven-membered cyclic **TS(12−13)** (−47.7 kcal/mol), including the hydrogen migrates from $AgHCO_3$ to C1 radical with simultaneously Ag transfers from C3 to carbonyl oxygen atom, which is fully consistent with experimental finding.[8] The spin density on C1/C3 changes from 0.95/0.03 of **12** to −0.07/0.92 of **13** in the protonation of C1, confirming the radical site transfers from C1 to C3 and the catalyst Ag_2CO_3 regenarates. Two pathways are considered in the protonation step of C3 radical by substrate **1** (path III-1a, **14** → **16**) or solvent **S** (path III-1b, **15** → **16**). Path III-1a (**TS(14−16)**) is slightly more favorable than path III-1b (**TS(15−16)**) by the relative free energy being 3.7 kcal/mol. This is the result of the stronger reactivity of C^{α}−H in **1**. Therefore, these two pathways are competetive processes. Then the intermediates **16** and **S**• are formed, and radical **4** is regenarated. As mentioned earlier, **S**• could react with **1** to obtain **4** and **S**. Besides, radical **4** could initiate **1** through self-initiation with $\Delta\Delta G^{\ddagger}$ value of 14.5 kcal/mol (Scheme S1). In path III-2, we investigated two pathways for the protonation of C1 radical with **1** (path III-2a) and **S** (path III-2b). Similar with path III-1, path III-2b (**TS(19−20)**) is slightly disfavored (1.8 kcal/mol) than path III-2a (**TS(18−20)**). Then C3 atom is protonated by $AgHCO_3$ via **TS(21−16)** with ΔG value of −47.3 kcal/mol to afford **16**. The comparison of the energy profile for paths III-1

DOI: 10.1021/acscatal.5b01703
ACS Catal. 2015, 5, 6177−6184

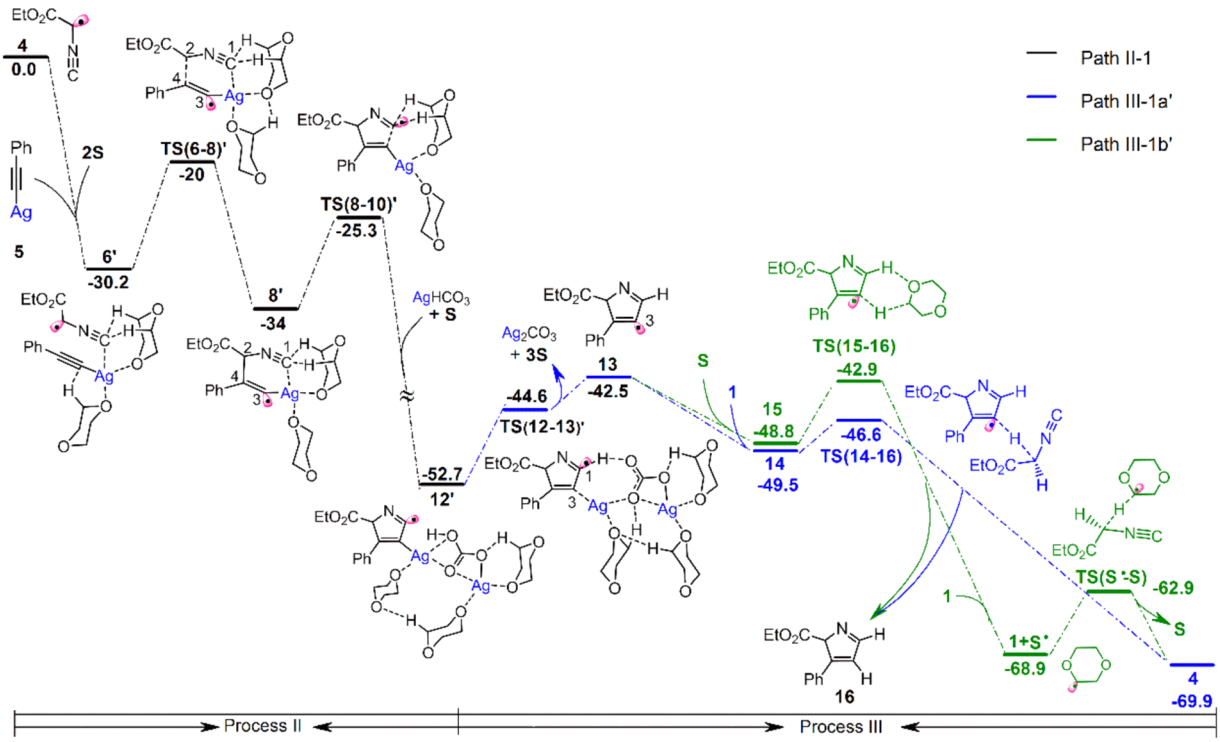

Figure 4. DFT-computed free-energy (ΔG_{sol}, in kcal/mol) profile for the most favorable pathway of processes II−III.

and III-2 suggests that path III-1 is dominant. Furthermore, the quantity of substrate **1** decreases as the reaction progresses; however, the bulk solvent can be recycled in the radical transfer process. Thereby, both **1** and **S** behave as radical/proton shuttle and catalyst in the concerted pronation and radical regenaration process III, facilitating the radical transfer extensively. To further optimize the reaction channel, we focused on path III-1 to inverstigate **S**-assisted paths III-1a′ and III-1b′ from intermediate **10**. As displayed in Figure 4, similar to previous results in processes I and II, the presence of **S** coodinating to Ag improves the reactivity by decreasing the activation barrier from 9.7 (**12** → **TS(12−13)**) to 8.1 kcal/mol (**12′** → **TS(12−13)′**) for the protonation of C1 radical.

The last process IV is the H-shift to generate the final product pyrrole. Herein the direct [1, 5]-H shift from C^{α} to N atom via **TS(16−Pr)** is kinetically unfeasible with high $\Delta\Delta G^{\ddagger}$ value of 30.7 kcal/mol. Considering the experimental fact that dioxane and isocyanide are the optimal solvent and a strong polar substrate, as well as trace water in the system, we investigated three possible pathways catalyzed by **S** (path IV-1), **1** (path IV-2), and water **W** (path IV-3), with varing numbers of participants 1−3, respectively. Nine models of complexation conformers are considered for 2−3 **S**/**1**-assisted cases (four conformations were found to be the most stable ones for different number of **S** and **1**; their structures and corresponding energies are presented in Figure S7). Each computed most stable complex is treated as the reference, respectively (Figures S6 and 5). Our calculated results suggest that each three-molecule cluster catalyst is the most favorable in reducing the barrier of [1, 5]-H shift process among combined clusters[31] (Figure 5, Table S3). The **S**-assisted H-shift is a stepwise deprotonation (via **TS(19c−19c′)**) followed by protonation (via **TS(19c′−Pr)**) process, while **1**-assisted H-shift occurs reversely, i.e., protonation (via **TS(18c−18c′)**), followed by the deprotonation (via **TS(18c′−Pr)**) process. However, the corresponding **W**-assisted one is a concerted step via seven-membered ring **TS(17c−Pr)**, which is less favorable than **1**- and **S**-assisted ones by 1.6 and 5.4 kcal/mol, respectively. Therefore, the **S**-assisted H-shift process is the most favorable one among these three-molecule-cluster-catalyzed pathways. The optimized structures of the key transition states are shown in Figure 6. This can be explained by the enhanced interactions (C−H···O, C−H···π, and C−H···N) and less ring strain of six-membered ring of **TS(19c−19c′)**. The detailed investigation of the last H shift process effectively clarifies the hydrogen source of N atom from C^{α}−H assisted by **S** serving as solvent and catalyst. Hence, solvent **S** and substrate **1** also act as catalysts and efficiently promote the whole reaction. We have recalculated the Gibbs free energies employing M06/SDD/6-311++G**/SMD method for optimizations of the rate-determining step (**6′** → **TS(6−8)′**). Compared with the results at the M06/SDD/6-311++G**(SMD)//B3LYP/LANL2DZ/6-31G level, the difference of activation barriers for **RDS** is 0.3 kcal/mol approximately ($\Delta\Delta G^{\ddagger}$ value for single calculation is 10.2 kcal/mol and that for the optimization is 9.9 kcal/mol), suggesting the current calculation level is reasonable and applicable in the current Ag-containing system.

For comparison, we carried out calculations at the same level of theory to explore the radical-free mechanisms proposed by Bi and Lei groups (Scheme 4, see details in SIiii-v). The calculated results indicate that the detailed reaction mechanism (M-I) proposed by Bi et al. mainly consists of five steps: the formation of silver−acetylide, isocyanide insertion to C−Ag bond, proton abstraction followed by intramolecular cyclization, H-shift, and protonation. Herein, **RDS** is the new C−C bond formation with a $\Delta\Delta G^{\ddagger}$ value of 29.8 kcal/mol at the isocyanide insertion step (**TS2−I**). For Lei's work, the reaction mechanism (M-II) involves the formation of silver-isocyanide and silver-acetylide simultaneously, intermolecular cyclization of the above two silver complexes, protonation, and H-shift.

DOI: 10.1021/acscatal.5b01703
ACS Catal. 2015, 5, 6177−6184

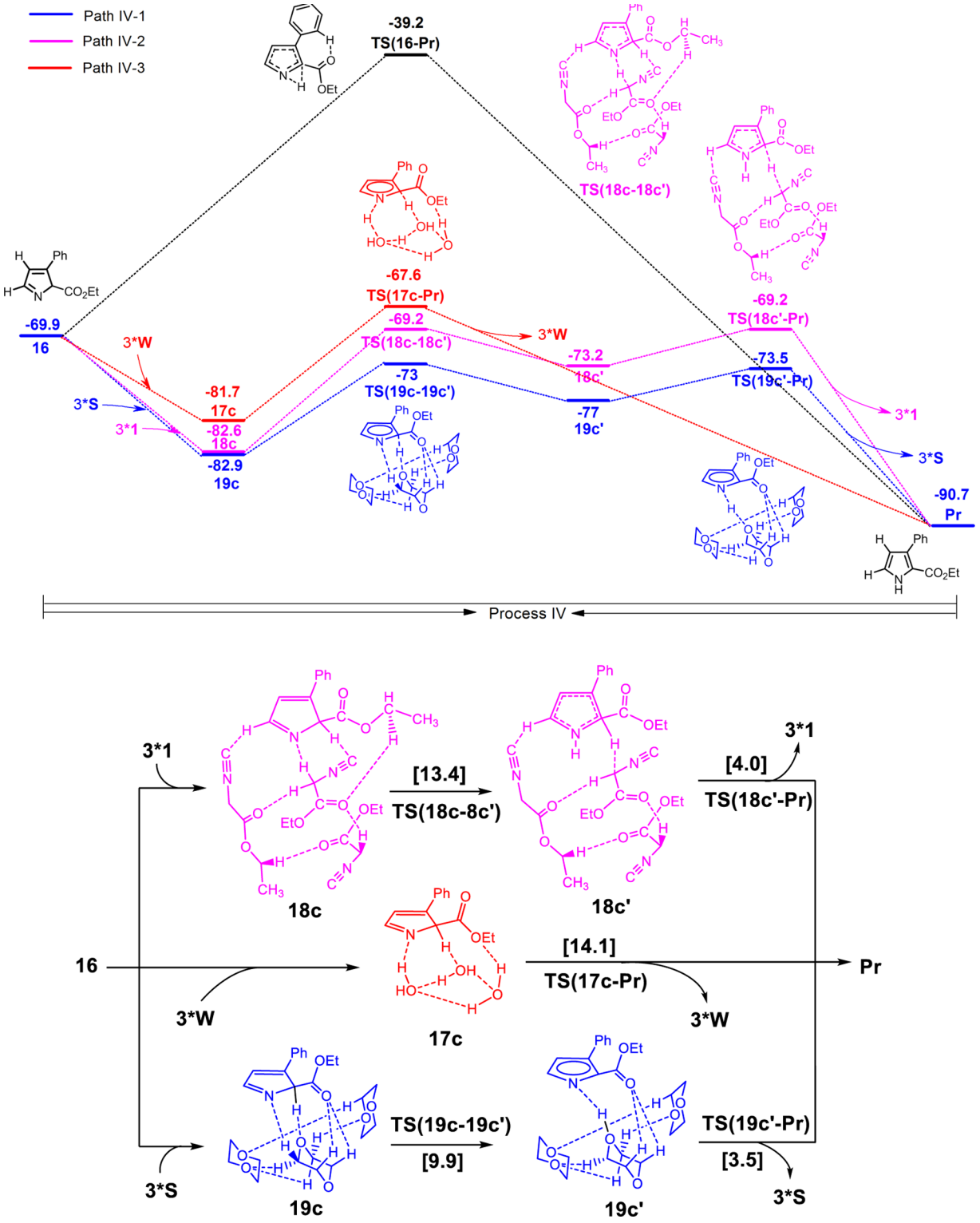

Figure 5. DFT-computed free-energy (ΔG_{sol}, in kcal/mol) profile and the structures of intermediates as well as transition states in each favorable three-**S**/**1**/**W**-assisted and direct H shift process IV.

RDS is the second protonation via **TS6−II** with a $\Delta\Delta G^{\ddagger}$ value of 40.3 kcal/mol. The inspection of the activation barriers of **RDS** for three investigated mechanisms clearly demonstrates that the $\Delta\Delta G^{\ddagger}$ value of **TS(6−8)′** of radical mechanism is the most favorable one by 19.6 and 30.1 kcal/mol compared to radical-free mechanisms **TS2−I** and **TS6−II**, respectively. Therefore, our computational results presented here may help elucidate the mechanism of such silver-catalyzed coupling or cyclization reactions.

CONCLUSION

In summary, we have performed DFT calculations and experiments to explore the detailed mechanism of isocyanide-alkyne cycloaddtion, especially the effect of reaction conditions

DOI: 10.1021/acscatal.5b01703
ACS Catal. 2015, 5, 6177−6184

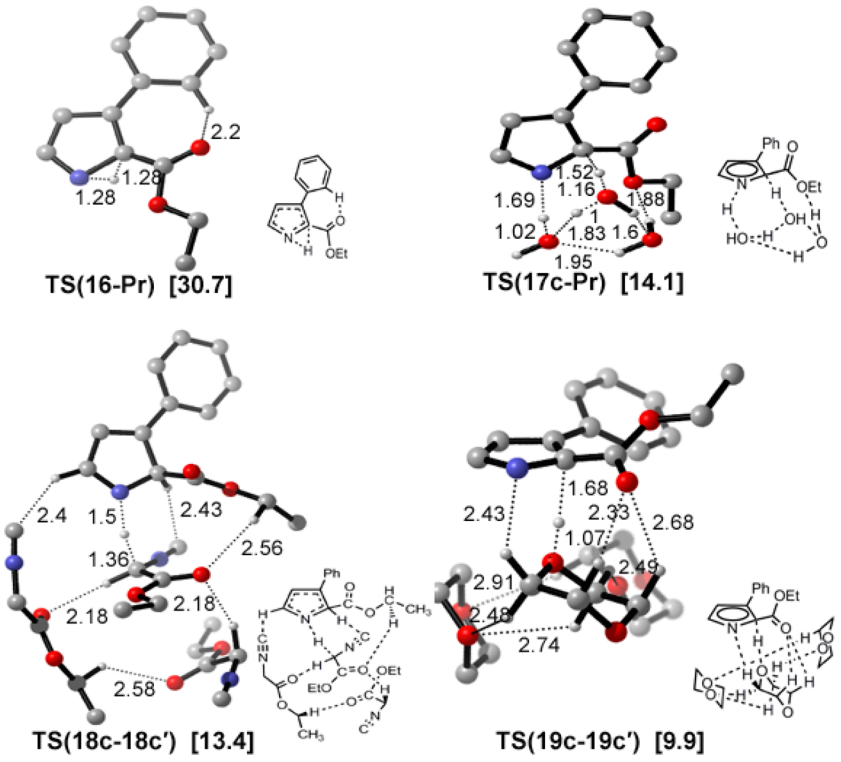

Figure 6. Optimized geometries of the key four transition states for the H-shift process. The corresponding activation barriers ($\Delta\Delta G^{\ddagger}$, in brackets) are in kcal/mol, and distances are in Å.

Scheme 4. Two Improved Unfavorable Radical-Free Mechanisms Proposed by Bi and Lei Groups at the Level of M06/SDD/6-311++G/SMD (1,4-Dioxane, 353.15 K)//B3LYP/LANL2DZ/6-31G****

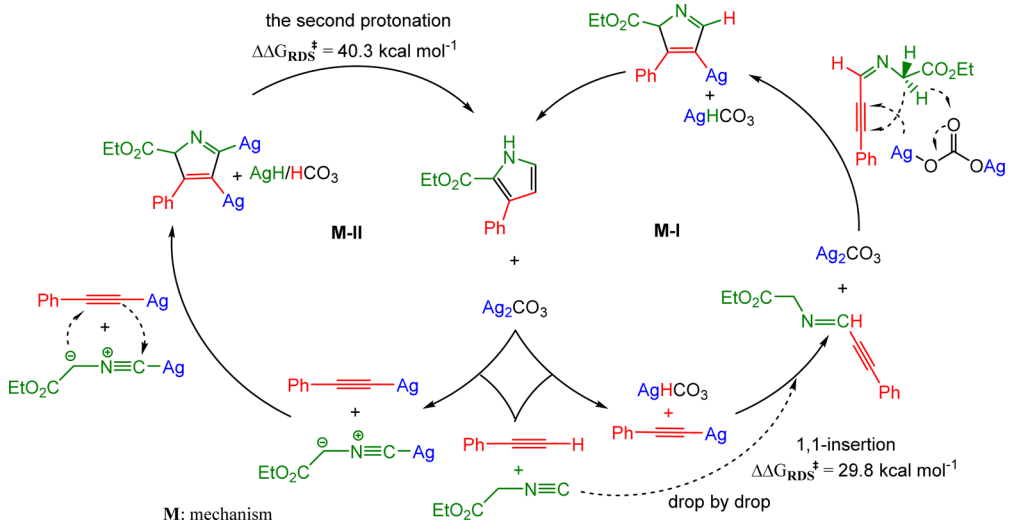

on mechanism. A novel radical mechanism was unraveled, employing multicatalysis of Ag_2CO_3, solvent, and substrate. Catalytic Ag_2CO_3 exposes double roles in the mechanism, i.e., serving as a unique base for the deprotonation of isocyanide and oxidant[12,23] to initiate the initial isocyanide radical formation. Then, it is found for the first time that substrate (isocyanide) and solvent (dioxane) can function as radical shuttle to regenerate radical for the next catalytic cycle, simultaneously completing the protonation. Furthermore, the participation of solvent dramatically improves the reaction activity by decreasing the activation barriers of the whole reaction, i.e., stabilizing the transition-state structures via Ag···O coordinations and C−H···O hydrogen bonds in Ag-containing processes as well as a much more efficient H-shift than in the substrate-/water-assisted and direct cases. These findings may open new insights for the mechanistic understanding of silver-catalyzed isocyanides or alkynes reactions, which in turn may provide guidelines for future design of synthetic methods.

■ ASSOCIATED CONTENT

Supporting Information

The Supporting Information is available free of charge on the ACS Publications website at DOI: 10.1021/acscatal.5b01703.

DOI: 10.1021/acscatal.5b01703
ACS Catal. 2015, 5, 6177−6184

Additional information for radical/radical-free mechanisms, experimental details, and XYZ coordinates (PDF)

AUTHOR INFORMATION

Corresponding Authors

*E-mail: jpzhang@nenu.edu.cn. Tel.: +86-431-85099372. Fax: +86-431-85099521.
*E-mail: bixh507@nenu.edu.cn.

Notes

The authors declare no competing financial interest.

ACKNOWLEDGMENTS

Financial support by the National Natural Science Foundation of China (21173037) is gratefully acknowledged.

REFERENCES

(1) (a) Baumgarten, M.; Tyutyulkov, N. *Chem. - Eur. J.* **1998**, *4*, 987−989. (b) Miyaji, H.; Sato, W.; Sessler, J. L. *Angew. Chem., Int. Ed.* **2000**, *39*, 1777−1780. (c) Yoon, D. W.; Hwang, H.; Lee, C. H. *Angew. Chem., Int. Ed.* **2002**, *41*, 1757−1759. (d) Ackermann, L.; Wang, L. H.; Lygin, A. V. *Chem. Sci.* **2012**, *3*, 177−180.

(2) (a) Perrin, D.; vanHille, B.; Barret, J. M.; Kruczynski, A.; Etievant, C.; Imbert, T.; Hill, B. T. *Biochem. Pharmacol.* **2000**, *59*, 807−819. (b) Lamberth, C.; Jeanmart, S.; Luksch, T.; Plant, A. *Science* **2013**, *341*, 742−746.

(3) (a) Estévez, V.; Villacampa, M.; Menéndez, J. C. *Chem. Soc. Rev.* **2010**, *39*, 4402−4421. (b) Ma, Z. Q.; Wang, X. L.; Wang, X.; Rodriguez, R. A.; Moore, C. E.; Gao, S. H.; Tan, X. H.; Ma, Y. Y.; Rheingold, A. L.; Baran, P. S.; Chen, C. *Science* **2014**, *346*, 219−224.

(4) (a) Sameiro, M.; Goncalves, T. *Chem. Rev.* **2009**, *109*, 190−212. (b) Brothers, P. J. *Inorg. Chem.* **2011**, *50*, 12374−12386. (c) Bauer, I.; Knölker, H. J. *Top. Curr. Chem.* **2011**, *309*, 203−253.

(5) (a) Estévez, V.; Villacampa, M.; Menéndez, J. C. *Chem. Soc. Rev.* **2014**, *43*, 4633−4657. (b) Xuan, J.; Xia, X. D.; Zeng, T. T.; Feng, Z. J.; Chen, J. R.; Lu, L. Q.; Xiao, W. J. *Angew. Chem., Int. Ed.* **2014**, *53*, 5653−5656. (c) Liu, Y. J.; Xu, H.; Kong, W. J.; Shang, M.; Dai, H. X.; Yu, J. Q. *Nature* **2014**, *515*, 389−393.

(6) (a) Larionov, O. V.; de Meijere, A. *Angew. Chem., Int. Ed.* **2005**, *44*, 5664−5667. (b) Lygin, A. V.; Larionov, O. V.; Korotkov, V. S.; de Meijere, A. *Chem. - Eur. J.* **2009**, *15*, 227−236. (c) Wang, Z. K.; Bi, X. H.; Liao, P. Q.; Liu, X.; Dong, D. W. *Chem. Commun.* **2013**, *49*, 1309−1311. (d) Wu, T.; Pan, L.; Xu, X. X.; Liu, Q. *Chem. Commun.* **2014**, *50*, 1797−1800.

(7) Gao, M.; He, C.; Chen, H. Y.; Bai, R. P.; Cheng, B.; Lei, A. W. *Angew. Chem., Int. Ed.* **2013**, *52*, 6958−6961.

(8) Liu, J. Q.; Fang, Z. X.; Zhang, Q.; Liu, Q.; Bi, X. H. *Angew. Chem., Int. Ed.* **2013**, *52*, 6953−6957.

(9) He, C.; Guo, S.; Ke, J.; Hao, J.; Xu, H.; Chen, H. Y.; Lei, A. W. *J. Am. Chem. Soc.* **2012**, *134*, 5766−5769.

(10) Schöllkopf, U.; Gerhart, F. *Angew. Chem., Int. Ed. Engl.* **1968**, *7*, 805−806.

(11) (a) Lygin, A. V.; de Meijere, A. *Angew. Chem., Int. Ed.* **2010**, *49*, 9094−9124. (b) Qiu, G. Y. S.; Ding, Q. P.; Wu, J. *Chem. Soc. Rev.* **2013**, *42*, 5257−5269.

(12) Daru, J.; Benda, Z.; Póti, Á.; Novák, Z.; Stirling, A. *Chem. - Eur. J.* **2014**, *20*, 15395−15400.

(13) (a) Wang, L.; Sha, W. X.; Dai, Q.; Feng, X. M.; Wu, W. T.; Peng, H. B.; Chen, B.; Cheng, J. *Org. Lett.* **2014**, *16*, 2088−2091. (b) Jin, J.; MacMillan, D. W. C. *Angew. Chem., Int. Ed.* **2015**, *54*, 1565−1569.

(14) Cheng, G. J.; Zhang, X. H.; Chung, L. W.; Xu, L. P.; Wu, Y. D. *J. Am. Chem. Soc.* **2015**, *137*, 1706−1725.

(15) (a) Krauter, C. M.; Hashmi, A. S. K.; Pernpointner, M. *ChemCatChem* **2010**, *2*, 1226−1230. (b) Xu, X. F.; Liu, P.; Shu, X. Z.; Tang, W. P.; Houk, K. N. *J. Am. Chem. Soc.* **2013**, *135*, 9271−9274.

(16) (a) Kovács, G.; Ujaque, G.; Lledós, A. *J. Am. Chem. Soc.* **2008**, *130*, 853−864. (b) Couce-Rios, A.; Kovács, G.; Ujaque, G.; Lledós, A. *ACS Catal.* **2015**, *5*, 815−829.

(17) (a) Xia, Y. Z.; Liang, Y.; Chen, Y. Y.; Wang, M.; Jiao, L.; Huang, F.; Liu, S.; Li, Y. H.; Yu, Z. X. *J. Am. Chem. Soc.* **2007**, *129*, 3470−3471. (b) Shi, F. Q.; Li, X.; Xia, Y. Z.; Zhang, L. M.; Yu, Z. X. *J. Am. Chem. Soc.* **2007**, *129*, 15503−15512. (c) Liang, Y.; Zhou, H. L.; Yu, Z. X. *J. Am. Chem. Soc.* **2009**, *131*, 17783−17785.

(18) Frisch, M. J.; Trucks, G. W.; Schlegel, H. B.; Scuseria, G. E.; Robb, M. A.; Cheeseman, J. R.; Scalmani, G.; Barone, V.; Mennucci, B.; Petersson, G. A.; Nakatsuji, H.; Caricato, M.; Li, X.; Hratchian, H. P.; Izmaylov, A. F.; Bloino, J.; Zheng, G.; Sonnenberg, J. L.; Hada, M.; Ehara, M.; Toyota, K.; Fukuda, R.; Hasegawa, J.; Ishida, M.; Nakajima, T.; Honda, Y.; Kitao, O.; Nakai, H.; Vreven, T.; Montgomery, J. A.; Peralta, J. E.; Ogliaro, F.; Bearpark, M.; Heyd, J. J.; Brothers, E.; Kudin, K. N.; Staroverov, V. N.; Kobayashi, R.; Normand, J.; Raghavachari, K.; Rendell, A.; Burant, J. C.; Iyengar, S. S.; Tomasi, J.; Cossi, M.; Rega, N.; Millam, J. M.; Klene, M.; Knox, J. E.; Cross, J. B.; Bakken, V.; Adamo, C.; Jaramillo, J.; Gomperts, R.; Stratmann, R. E.; Yazyev, O.; Austin, A. J.; Cammi, R.; Pomelli, C.; Ochterski, J. W.; Martin, R. L.; Morokuma, K.; Zakrzewski, V. G.; Voth, G. A.; Salvador, P.; Dannenberg, J. J.; Dapprich, S.; Daniels, A. D.; Farkas, O.; Foresman, J. B.; Ortiz, J. V.; Cioslowski, J.; Fox, D. J. *Gaussian 09*; Gaussian, Inc.: Wallingford, CT, 2009.

(19) (a) Becke, A. D. *J. Chem. Phys.* **1993**, *98*, 5648−5652. (b) Becke, A. D. *J. Chem. Phys.* **1993**, *98*, 1372−1377.

(20) (a) Roy, L. E.; Hay, P. J.; Martin, R. L. *J. Chem. Theory Comput.* **2008**, *4*, 1029−1031. (b) Bagno, A.; Bonchio, M. *Chem. Phys. Lett.* **2000**, *317*, 123−128.

(21) Zhao, Y.; Truhlar, D. G. *Theor. Chem. Acc.* **2008**, *120*, 215−241.

(22) Krishnan, R.; Binkley, J. S.; Seeger, R.; Pople, J. A. *J. Chem. Phys.* **1980**, *72*, 650−654.

(23) Yang, Y. F.; Cheng, G. J.; Liu, P.; Leow, D. S.; Sun, T.-Y.; Chen, P.; Zhang, X. H.; Yu, J. Q.; Wu, Y. D.; Houk, K. N. *J. Am. Chem. Soc.* **2014**, *136*, 344−355.

(24) Gonzalez, C.; Schlegel, H. B. *J. Phys. Chem.* **1990**, *94*, 5523−5527.

(25) Marenich, A. V.; Cramer, C. J.; Truhlar, D. G. *J. Phys. Chem. B* **2009**, *113*, 6378−6396.

(26) Yang, H.; Wong, M. W. *J. Am. Chem. Soc.* **2013**, *135*, 5808−5818.

(27) Lu, T.; Chen, F. W. *J. Comput. Chem.* **2012**, *33*, 580−592. Available at: http://multiwfn.codeplex.com (accessed August, 2013).

(28) Legault, C. Y. CYLview, 1.0b; Université de Sherbrooke: Sherbrooke, **2009**. Available at: http://www.cylview.org (accessed September, 2014).

(29) (a) Kozitsyna, N. Y.; Nefedov, Y. A.; Kochubey, D. I.; Klyagina, A. P.; Markov, A. A.; Dobrokhotova, Z. V.; Velikodny, Y. A.; Zyubina, T. S.; Gekhman, A. E.; Vargaftik, M. N.; Moiseev, I. I. *Inorg. Chim. Acta* **2011**, *370*, 382−387. (b) Neo, Y. C.; Vittal, J. J.; Hor, T. S. A. *J. Chem. Soc., Dalton Trans.* **2002**, 337−342.

(30) Cao, J. J.; Zhu, T. H.; Wang, S. Y.; Gu, Z. Y.; Wang, X.; Ji, S. J. *Chem. Commun.* **2014**, *50*, 6439−6442.

(31) (a) Zheng, Y. Y.; Zhang, J. P. *ChemPhysChem* **2010**, *11*, 65−69. (b) Yuan, H. Y.; Zheng, Y.; Zhang, J. P. *J. Org. Chem.* **2012**, *77*, 8744−8749. (c) Yuan, H. Y.; Zheng, Y. Y.; Fang, Z. X.; Bi, X. H.; Zhang, J. P. *Green Chem.* **2014**, *16*, 2653−2663.

DOI: 10.1021/acscatal.5b01703
ACS Catal. 2015, 5, 6177−6184